

# DESIGN AND REALIZATION OF A LIGHTWEIGHT MECHANICAL DRIVETRAIN FOR AN ELECTRIC FORMULA STUDENT RACECAR

Hannah Daled<sup>1</sup>, Raf Schoenaers<sup>1</sup>

<sup>1</sup> Master student Electromechanical Engineering,  
Faculty of Engineering Technology, Campus Group T, Leuven  
Vesaliusstraat 13, 3000 Leuven, Belgium

Supervisor: prof. ir. Guido Ceulemans  
Unit Energy  
Faculty of Engineering Technology, Campus Group T, Leuven  
Vesaliusstraat 13, 3000 Leuven, Belgium  
guido.ceulemans@kuleuven.be

Co-supervisor: Giannino Bortolini  
Drive Technology, SEW-EURODRIVE, Evenementenlaan 7, Researchpark Haasrode 1060

## ABSTRACT

This master's thesis is about the design and realization of two transmissions for Formula Group T's 2014 Formula Student racing car, June. Formula Group T is a team of 22 engineering students who take part in the Formula Student competition. Because of the very tortuous Formula Student circuits, June has to be very agile and light. That is why the drivetrain consists of two separate electric motors and why we set the ambitious goal of a maximum weight of 5 kg for both transmissions. Apart from the weight we also had to make well thought out compromises concerning cost, production, ease of assembly, partners, size, future ambitions of the team and reliability. The epicyclic reduction in planet configuration proved to be the lightest design amongst a comparison of four different transmission types. The load distribution among the three planet gears results in a very lightweight and compact transmission. The bottleneck which limits the compactness of the epicyclic reduction is the outer diameter of the planet gear. Therefore, we went through an iterative design process to design the transmission as light as possible. The result is an epicyclic gear reduction in planet configuration weighing 2,2 kg per transmission, a weight reduction of 75% compared to last year's transmission.

## Keywords

Formula Student Electric, Formula Group T, epicyclic gear reduction, planetary reduction, mechanical drivetrain, lightweight transmission.

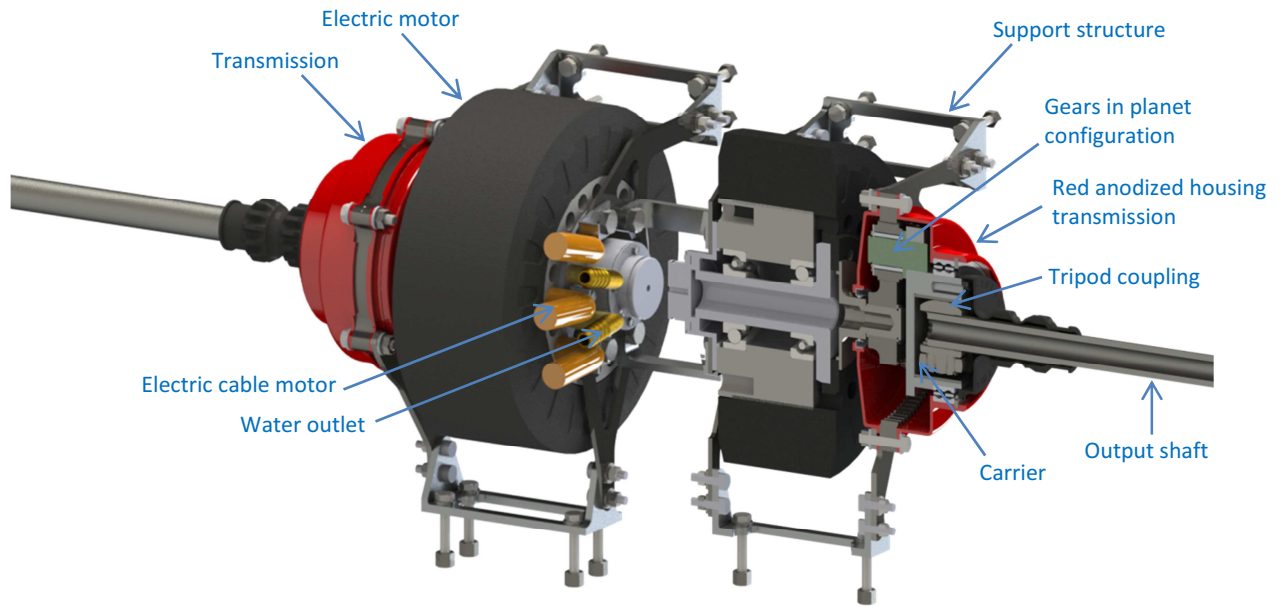


**Figure 1.** Render of the final design, the right motor and transmission assembly is cut in half to show the inner workings

## 1 INTRODUCTION

This paper describes the design of the transmission of Formula Group T's<sup>[1]</sup> 2014 Formula Student racing car called June. Formula Group T is a team of 22 engineers who take part in the Formula Student<sup>[2]</sup> competition: Europe's most established educational motorsport and engineering competition, providing testing ground for the next generation of world class engineers. During summer break Formula Group T will participate in three official competitions. June is Formula Group T's third car, the successor of Eve. The latter was a huge step forward in all areas. Her drivetrain is composed of two electric motors, one for each rear wheel. Since each rear wheel has its motor, an electronic differential is implemented and improves the agility, but will not be discussed in this master's thesis.

A competition always consists of static and dynamic events, where you can get a maximum of respectively 325 and 675 points. The points are assigned using the distribution shown in table 1.

**Table 1.** Scoring Formula Student competition

Static Events:	
Presentation	75
Engineering Design	150
Cost Analysis	100
Dynamic Events:	
Acceleration	75
Skid-Pad	50
Autocross	150
Efficiency	100
Endurance	300
Total Points:	1000

To gain as much points as possible at the Formula Student competitions, we first defined our main targets concerning the design of our transmission.

In section 2 we explain the targets of our design and of this master's thesis. The two main goals are the design of a lightweight transmission and to finish the design and implementation in no more than nine months. The distinct motor design had some influence on the design of the transmission, which is why we explain our motor choice in section 3. Subsequently, we determined the optimal transmission ratio of 3,52. The motor design, the motor torque, maximum speed and transmission ratio provides the basis to determine the most suited transmission: we designed several transmission types, detailed enough to make a substantiated decision. The comparison included a chain drive, a belt drive and a transmission with spur gears.

The most optimal design is the epicyclic gear reduction. The absence of radial forces on the motor shaft and the power distribution among the three planet gears are the two main reasons of the low weight, our main goal. The structure to mount the motor and the epicyclic gear reduction is mainly subjected to the driving and reaction torque as can be found in section 11. This load case is ideal to design a very lightweight support structure. And finally, the compact size results in a very compact design of the monocoque, which again results in a lighter car. For a transmission ratio of 3,52 the epicyclic gear reduction in planet configuration is the lightest solution. In section 6 we explained the difference with the star configuration and why the latter will be heavier.

Once we found the best solution for our application, we focussed on the bottleneck: the planet gear. The planet gear is the smallest gear and contains a shaft and a bearing that has to transmit one third of the output torque of 440 Nm. The optimization process of the planet gear,

the shaft and the bearing is an iteration where all these parts are designed simultaneously, as can be found in section 7 and 8. The three shafts of the planet gears (called 'carrier pins') are press fit into the carrier. This press fit connection is crucial because the aluminum carrier has a higher thermal expansion coefficient than the steel carrier pins. That is why we dedicate the entire section 9 to this important calculation.

Section 10 and 11 will discuss the design of the spline connection of the motor shaft and the sun gear with a radial clearance to ensure an equal load distribution among the three planet gears. This optimal load distribution also influences the design of the support structure, where both weight and cost issues are taken into consideration. An important check is carried out concerning the temperature of the transmissions because of the high power density. Based on logs during testing, we set up the load case, calculated the total power loss and determined the transmission temperature. We obtain a maximum temperature of  $58^{\circ}\text{C}$ , which is less than the maximum allowed  $80^{\circ}\text{C}$ : the temperature at which the oil seal will be damaged.

The result of this paper is a transmission with a weight reduction of 75% compared to our previous transmission in Eve. A set of epicyclic gears in planet configuration turned out to be the best design for our criteria with a total weight of around 2,2 kg per gearbox.

## 2 DESIGN CONSTRAINTS AND GOALS

In figure 1 we provide an overview of the main components of the transmission. The basis for this final design is the goals we want to achieve and the design restrictions we encounter.

Our own goals:

- Based on what we learned from transmissions of other teams and our experience of last year, we set the ambitious goal of a weight of only 2,5 kg per transmission which will position our transmission among the lightest of the competition.
- The transmissions should be easy to assemble and to disassemble.
- Compact, to reduce the size and thus the weight of the monocoque.
- Every mechanical drivetrain component should be sponsored.
- Each rear wheel has to be powered by a separate motor to be able to implement an electronic differential.
- Design, production and implementation within a time period of nine months.

Formula Student rules<sup>[3]</sup> restrictions:

- By regulations, the total power of the drivetrain is limited to 85 kW.
- Pass a tilt-test at the competition to ensure that no fluids will spill from the car under heavy cornering. The racecar is tilted sideways over a  $60^{\circ}$  angle during this test.

## 3 MOTORS

To obtain a lightweight drivetrain it is crucial to have a motor with a high torque to weight ratio. Motor developer Enstroj supplies a pancake axial flux synchronous motor with an outer rotor, shown in figure 4: the water cooled EMRAX 207.

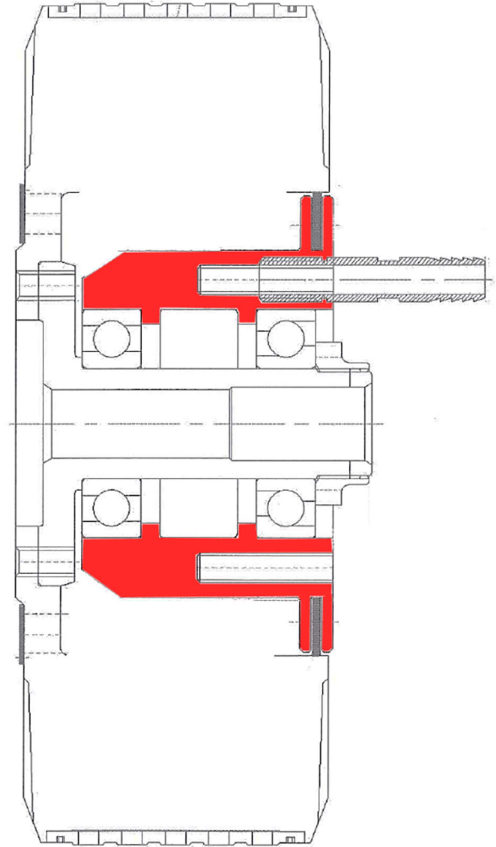


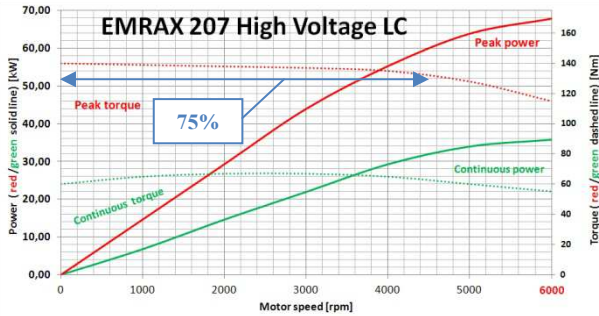
**Figure 2.** Section view EMRAX 207<sup>[4]</sup>, stator indicated in red is only accessible at one side of the motor

This motor has a high peak torque of 160 Nm and a peak power of 70 kW. The specifications of the motor together with the fact that we have experience with this type and the price made us choose it.

To make full advantage of the superior controllability of electric motors the drivetrain will consist of two motors, one for each rear wheel. By implementing an electronic differential we save the weight of a mechanical differential and we can control the torque on each rear wheel separately. This improved controllability results in a more agile car and consequently in lower lap times given the very small and tortuous circuits of the Formula Student competition. The electronic differential falls outside the scope of this master's thesis.

The principle of the outer rotor influenced the design of the entire transmission. On the section view depicted on figure 2, it can be seen that the only stationary component is the stator indicated in red. The stator is only accessible at one side of the motor and contains the high voltage cables and cooling outlets. In the section 5, where we consider various transmission concepts, this

unusual motor design will have its influence on the evaluation of the concepts.



**Graph 1.** Torque and power characteristic EMRAX 207; peak torque is constant up to about 4500 rpm

Intrinsically, electric motors have their peak torque available at standstill. This torque is constant up to about 75% of the maximum speed as shown in graph 1. That is why we do not need to shift between a number of transmission ratios to continuously operate at maximal torque. The next step is to find out the optimal transmission ratio to reduce the motor speed and to increase the driving torque which is discussed in the next section.

#### 4 TRANSMISSION RATIO CALCULATION

To calculate the transmission ratio we use the maximum torque we can apply at each rear wheel without slipping which is 440 Nm. This value is a result of research performed by a former team member who composed a vehicle dynamics model with implementation of a custom tire model<sup>[5]</sup>. We calculate the transmission ratio based on this maximum torque value and afterwards check the maximum speed. The reason we check this is the following: at the acceleration event we have to accelerate as fast as possible over a distance of 75m and the top speed should not be reached before the finish line. At a top speed of 160 km/h we are sure this is not the case and we determine the transmission ratio at 3,52. With the transmission ratio and motor secured we are now able to make a decent comparison between different transmission concepts.

#### 5 DIFFERENT CONCEPTS

To determine which reduction concept is the most appropriate for our application we compose a decision matrix where we grade four transmission concepts based on different criteria (appendix X). The concepts we consider are spur gears, chain drive, toothed belt drive and a planetary transmission. We first draft a list of 19 criteria, from which we extract six parameters which are the most important in our design and application. The most important criterion is the weight followed by volume, overloading, optimization, pre-tensioning and efficiency. We assign a weight factor to each criterion: a high weight factor means an important criterion. We provide an overview in table 2. We calculate a total per

concept, which is the weighted sum of the score on each criterion.

**Table 2.** Six decision criteria with an assigned weight factor. Per concept a total score is calculated: the weighted sum of each criterion.

Criteria	Gears	Epicyclic	Chain drive	Toothed Belt Drive	Weight Parameter
1 Weight	3	5	3	3	4
2 Volume	3	5	3	1	4
3 Overloading	5	5	4	2	4
4 Optimize	5	5	3	3	3
5 Pre-tensioning	5	5	4	2	3
6 Efficiency	5	4	3	4	3
<b>TOTAL</b>	89	102	70	51	

Before we start our comparison we will explain in short why these criteria are important for us:

1. Low weight is a crucial aspect of our design: the lighter the car, the faster and the better the dynamics are.
2. The volume of the drivetrain is also related to weight: a smaller drivetrain results in a more compact monocoque, which is again a weight reduction for the car.
3. The overload criterion is less obvious: a design which can withstand a certain amount of overload can be made 'less strong' and thereby lighter.
4. Optimization is a criterion to indicate how much we can optimize the design for our specific application. When buying standard parts they are often too heavy and are less appreciated by the design judges on the Formula Student competition.
5. Pre-tensioning is the fifth criterion, designs that need pre-tensioning are chain and belt drives. The pre-tensioning device adds weight, complicates the design and adds useless stresses.
6. We have chosen the efficiency of the transmission as the final criterion since the efficiency of the racecar is measured at the competition and makes up 10% of the total points.

To assign values for each transmission concept for the six parameters we made a rough design of each possible concept, starting with the spur gears.

##### 5.1 Spur gears

The advantages of a spur gear reduction are that it is a pretty straightforward design, almost each component can be custom designed by ourselves, the efficiency of spur gears is quite high and no pre-tensioning is needed. We would place the gear reduction for both motors in the centre in a shared housing, this way we can save weight and reduce the number of milled parts. We calculated the total weight would probably be around 5 kg. One major disadvantage is that the design takes up quite some space, as you can see in figure 3.



**Figure 3.** Visual comparison of the three concepts, from left to right: epicyclic gear reduction, spur gear and timing belt

## 5.2 Toothed belt drive

The second concept we took a closer look at is the toothed belt drive. Based on Gates belt catalogue<sup>[6]</sup> we calculated some realistic parameters of the design of a toothed belt drive for our application. We calculated the effective force, the pre-tensioning force and the force in the tight side of the belt. For these calculations we had to use the maximum load values the reduction will endure, because a belt drive cannot be overloaded. These values lead to belt type ATL10. We also have to take rule T8.4.4 and T8.4.5 of the Formula Student rules<sup>[3]</sup> into consideration which specifies the material and dimensions of obligatory metal scatter shield for a non-metallic belt drive. This all leads to a total expected weight of yet again around 5 kg. The volume the toothed belt concept takes up is a very prominent disadvantage, as you can see in figure 3.

## 5.3 Chain drive

The third concept was a chain drive. To get an idea of the dimensions of a chain drive we followed a standard design procedure method as described in Roloff/Matek, which you find in appendix 3. Again we are obliged by the Formula Student rules to include a metal scattershield for each chain, which leads to a total weight of around 6 kg.

## 5.4 Epicyclic gear reduction

The final transmission concept we considered is the epicyclic gear reduction, which came out as the clear winner of our decision matrix in table 2. This concept holds a lot of advantages. It is a very compact design because the power is distributed among three planet gears and the absence of radial forces on the motor shaft leads to a light mounting structure. The coaxiality of the motor shaft and the driven shaft improves the compactness of the drivetrain vastly. The one disadvantage we come across is that the temperature might be a lot higher, due to the multiple meshes and high power density. The temperature is discussed more in depth in section 12. The design is also quite difficult, so we really needed to find the right company with the appropriate knowledge to assist us, which luckily we found in SEW-EURODRIVE.

The decision for the planetary gear reduction was supported by the long-term vision of the team to evolve towards building a racecar with four-wheel drive, with

in-wheel planetary gearboxes, so this thesis is the perfect base for future team members with regards to knowledge and contacts with companies. The advantages and set up of the epicyclic design will be discussed more in-depth in the next section.

## 6 EPICYCLIC REDUCTION

In this section we clarify the advantages of the epicyclic gear reduction and the reasons behind its low weight. On figure 4 all radial forces caused by tooth geometry are indicated. It is clear that there is no resulting radial force acting on the motor shaft in the centre. Note that this is only true when there is an equal load distribution among the planet gears. This important requirement will be discussed in section 10 about designing the spline connection. The absence of a resulting radial force allows us to design a lightweight support structure that only has to resist the reaction torque acting on the gearbox. It is easier to design a lightweight support structure for one type of load. This design can be found in section 11 about the support structure.

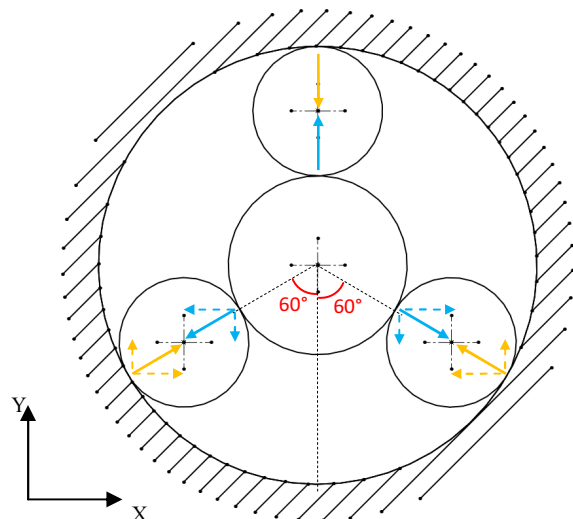


**Figure 4.** Radial forces in an epicyclic gear reduction. Continuous arrow: radial force, dotted arrow: x or y component of the radial force. Input: sun gear, output: carrier.

The ratio of 3,52 can be achieved by two different configurations of the epicyclic gear reduction: a star and

a planet configuration. The configuration depends on which component is driven, driving and fixed. Figure 5 and 6 provide a schematic overview of both configurations.

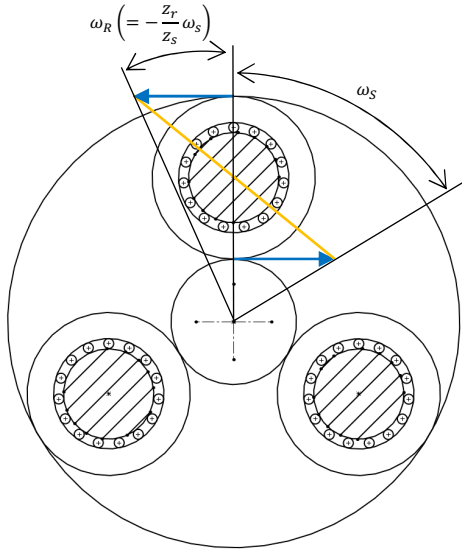


**Figure 5.** Schematic representation of the star configuration: the sun gear is the input, the carrier is fixed and the ring gear is the output. The relative speeds visualize the transmission ratio.

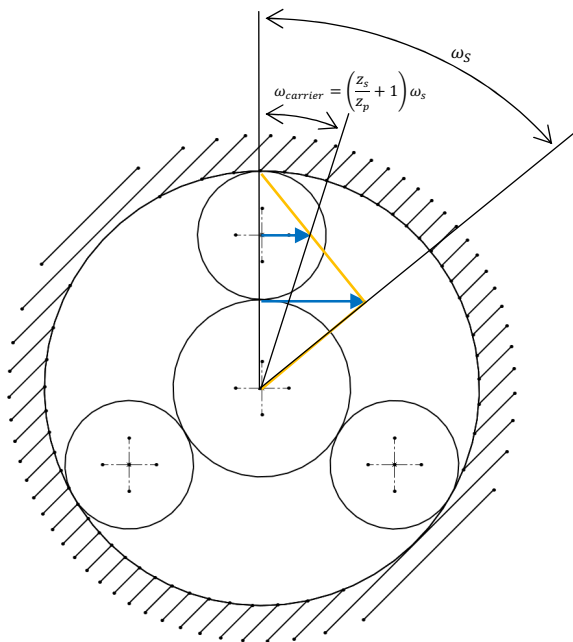


**Figure 6.** Schematic representation of the planet configuration: the sun gear is the input, the ring gear is fixed and the carrier is output. The relative speeds visualize the transmission ratio.

The most relevant differences between these two configurations are the reaction torque acting on the gearbox and the diameters of the planet gears. The epicyclic gear reduction in planet configuration turns out to be the best choice to meet our lightweight design goal. This conclusion is based on the effect of the reaction torque and pin diameter on the weight of the gear reduction:

- The first main difference is the reaction torque acting on the housing of the gearbox, and thus acting on the support structure. To obtain the reaction torque acting on the gearbox we compose the free body diagram of both the planet and the star configuration, which can be seen on figure 7 and 8 respectively. An in-depth discussion can be found in appendix 5. The reaction torque of the star configuration is 565 Nm, while the reaction torque of the planet configuration is only 315 Nm. This will result in a heavier epicyclic gear reduction and support structure.
- The second big difference is the diameter of the planet gears, which is the bottleneck of the weight reduction. Because the diameters of the planet gears in the star configuration are larger in comparison to the sun gear, there is more room to install the bearing and the pin inside. This advantage is downplayed by the high reaction torque which requires the pins inside the planet gears to be larger and thereby heavier.

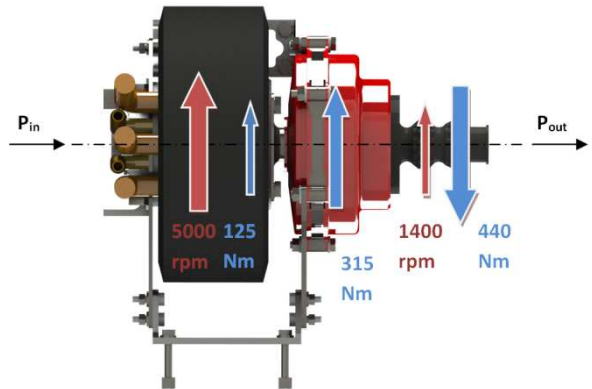


**Figure 7.** Free body diagram planet configuration: a reaction torque of 315 Nm acts on the gearbox and its support structure

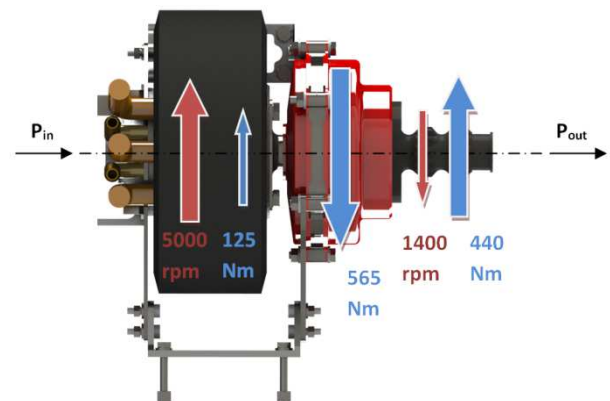


**Figure 8.** Free body diagram star configuration: a reaction torque of 565 Nm acts on the gearbox and its support structure

After having determined the transmission ratio, the transmission type and the specific configuration, we now design the epicyclic gear reduction itself. The design starts with an iterative procedure to determine the lightest set of gears together with the needle bearings inside the planet gears.

## 7 GEARS

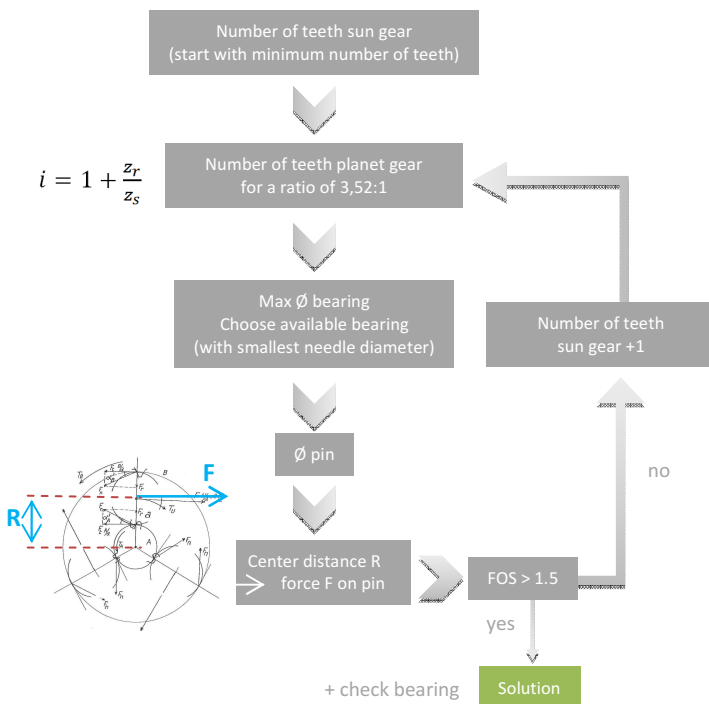


**Figure 9.** Flowchart to determine number of teeth

To calculate the dimensions of the gears we compose a flowchart which you see in figure 9. We start with a sun gear with 17 teeth<sup>[7]</sup>, the minimum number to avoid undercutting of the tooth flank. Using the formula for the transmission ratio<sup>[8]</sup> and the previously determined ratio of 3,52, we know the number of teeth of the ring gear. Next we use the first condition for planetary gear systems to determine the number of planet gear teeth:  $z_{ring} = z_{sun} + 2z_{planet}$ <sup>[8]</sup>.

The planet gears are idle gears, what means that each tooth endures two loads per revolution, both loads act in opposite direction. It is obvious that a tooth is only strong enough if there is enough material below the dedendum circle. According to DIN 3990 there should be material at least 3,6 times the modulus below the dedendum circle. Additionally the planet gears are made 3 mm wider than the sun gear and the ring gear to make the teeth more resistant against bending on top of a positive profile shift.

By respecting the DIN 3990 norm we now know the maximum diameter of the needle bearing we can insert into the planet gear. In the catalogue of FAG<sup>[9]</sup> we choose an available needle bearing, which gives us a value for the outer diameter of the carrier pin inside the planet gear. We calculate the force on this carrier pin based on the number of teeth of the planet gear, the modulus and the torque input from the motor. Next we simulate this force on the pin in SolidWorks and if the factor of safety is larger than 1,5 we accept the dimensions of the gears, otherwise we add one tooth to the sun gear and repeat the process. The result was 40 teeth for the sun gear, 29 for each planet gear and 101 for the ring gear.

The next step is to use KISSsoft to calculate the gears, the output files can be found in appendix 18. After this

SEW-EURODRIVE and VCST checked the gear calculations. Finally the gears are verified one more time according to a standard design procedure as described in Roloff/Matek<sup>[10]</sup>, where the tooth strength and the contact strength is checked [appendix 6b].

Because our gear manufacturer VCST produces the majority of their products in 16MnCr5, we choose the same material for financial reasons. In picture 10 you can see the final result of the gears. After the design of the gears we have to check if the bearings can bear the load, which is discussed in the next section.



**Picture 10.** Photo of the produced gears

## 8 BEARINGS

There are two types of bearings present in the epicyclic transmission, both indicated in figure 11:

- Inside the planet gear is a needle bearing k18x24x20 provided by FAG, which is a bearing with a cage. Our choice for a needle bearings inside the planet gear is obvious, since needle roller bearings have two to eight times the load-carrying capacity per given mass than any other bearing type<sup>[11]</sup> and that is exactly what we need for a compact and light design. Although the load capacity of a full complement needle bearing (only consisting of loose needles, without a cage) is higher, we opted for the needle bearing with a cage to simplify the assembly and disassembly of the transmission. The carrier pin and the bore of the planet gear provide the running surfaces for the needle bearing.
- The second bearing is a sealed angular contact double row ball bearing 3814-B-2RSR-TVH, located around the integrated tripod housing part of the carrier as you can see in figure 12. This bearing is an O-configuration to provide a stiff support for the carrier. Despite the very limited axial load, the bearing is axially secured in both directions. The only axial load that can occur is the movement of the drive shaft during cornering.

We want to notice the absence of a bearing around the motor shaft. Since there is no resulting radial force acting on the motor shaft we do not have to support it, we only

have to provide an oil seal. This avoids a hyperstatic motor shaft as the motor already has two bearings inside.

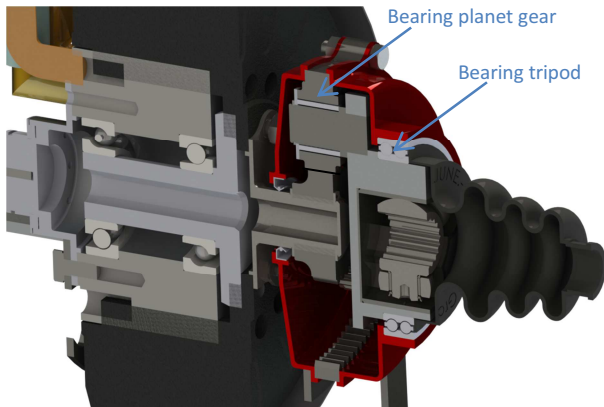
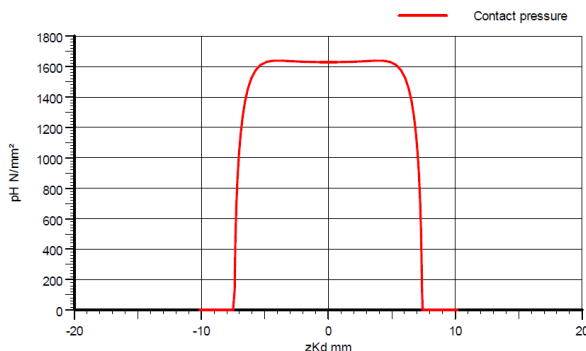


**Figure 11.** Indication of the bearing locations in the transmission

To simulate the bearings we use BEARINX®-online Shaft Calculation, provided to us by Schaeffler, our bearing supplier. We use a load cycle of 90% nominal (75 Nm, 2500 rpm) and 10% peak (125 Nm, 5000 rpm) as input. This load cycle was based on logs made on last year's car Eve and competition results, more information on how this load cycle was constructed can be found in appendix 7a. The output values that are particularly interesting to us are the contact pressure and the kappa value, which will be discussed below.

### 8.1 Contact pressure

For the needle bearing the maximum occurring contact pressure is 1538 N/mm<sup>2</sup>, this maximum pressure occurs where the carrier pin and the needles make contact. A contact pressure between 1500 and 1800 N/mm<sup>2</sup> means the bearing is slightly reduced in lifetime, but because our value is only slightly above the 1500 N/mm<sup>2</sup> limit and only occurs 10% of the time (peak torque and rpm), we approach the ideal theoretical infinite lifetime. Because the resulting radial force on the carrier is zero, the software does not calculate a contact pressure for the double row ball bearing; it is safe to assume this gear also approaches theoretical infinite lifetime.



**Graph 2.** Contact pressure on needle bearing, output from BEARINX®-online Shaft Calculation

In graph 2 you can see that the contact pressure is equally distributed along the length of the needle bearing, the

absence of peak values means there is no concern for tilting of the needles.

### 8.2 Kappa value

The kappa value, also known as the viscosity ratio  $\kappa$ , is related to the film thickness of the lubrication between the rolling element and the bearing surface. Typically there are three situations that can occur, which can be observed in figure 12: the friction coefficient in function of the layer thickness of the lubricant which depends on the viscosity of the oil, the speed of the bearing and the load on the bearing.

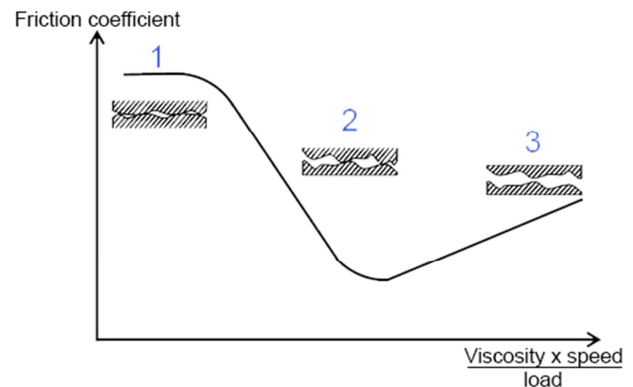


**Figure 12.** The friction coefficient in function of the layer thickness of the lubricant which depends on the viscosity of the oil, the speed of the bearing and the load on the bearing. 1: metal/metal contact, 2: very thin lubricant layer with almost but no metal/metal contact, 3: thick lubricant layer<sup>[12]</sup>

The first situation with metal/metal contact is not desirable since this will generate high friction which will cause heat. This heat will warm up the rolling elements which will reduce the lifetime of the bearing. The third situation is not desirable as well. The thick layer of lubricant between the rolling element and the bearing surface will lead to churning losses in the lubricant. Churning losses can be considered as hydrodynamic friction. They will heat the lubricant, causing the bearing to heat and hence reduce the lifetime of the bearing.

According to the principles described by Schaeffler a kappa value of  $\kappa = 3$  to 4 will lead to a very long lifetime. However, highly viscous oils cause additional power losses due to the churning losses. We should aim for a kappa value of around 2, a requirement which both of the bearings satisfy.

In the next section we take a closer look at the steel carrier pins the needle bearings run around, and the construction of the carrier which holds the three carrier pins with planet gears in place.

## 9 CARRIER

For the production of the carrier we considered different production methods. We decided on milling the aluminum carrier, turning the steel pins and connecting the pieces by press fitting the pins into the carrier to achieve the lightest carrier possible. Another possibility is to produce the carrier and pins as one single heavy steel piece but the problem here is that we would need a



special tool to turn the pins to the correct tolerance. These are very high tolerances because the surface of the pin is also the running surface for the needle bearing.

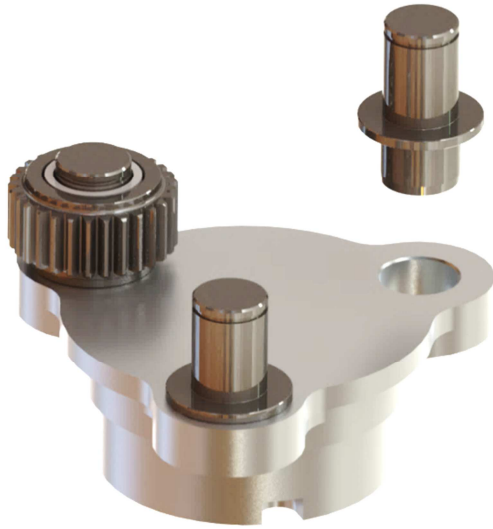


**Figure 13.** Render of the carrier and pressed pins

When calculating the press fit we consider three temperatures at which the stresses may not become too high:

- The first temperature is at 20°C, when the transmission is at room temperature.
- The second is at 120°C. This is an exaggerated worst case scenario since in fact the transmission temperature should never be higher than 80°C because of the oil seals, see section 12. When the temperature increases the aluminum expands more than the steel pin and the press fit will become loose. Under all circumstances the carrier pins must always have enough interference with the aluminum hole to transmit one third of the forces, who are responsible for the driving torque of 440 Nm.
- We also considered the opposite extreme: when the racecar has to spend the night outside at -20°C, the aluminum carrier will shrink more than the carrier pins, which will increase the interference and hence the stresses. Again, the stresses may not become higher than the yield stress of aluminum.

We decided for the carrier pin on tolerances of  $19_{+0,055}^{+0,060}$  mm and for the hole on  $19_{-0,000}^{+0,010}$  mm. We use SolidWorks to simulate this press fit and afterwards validate them by calculating the chosen press fit output values ourselves. We approach it as a press fit of a shaft in a thick walled cylinder as described in Fundamentals of Machine elements<sup>[13]</sup>. Table 3 is an overview of the input values: the internal diameter of the holes in the aluminum 7075-T6 carrier with their tolerance, Poisson's ratio, Young's modulus and the roughness. The table contains analogue input parameters for the pin which is made from steel alloy

16MnCr5. The length of the pin that is pressed in is 12 mm. For the coefficient of friction we select an interval from 0,10 to 0,15.

**Table 3.** Input values for the press fit calculation

		Case 1 @20°C	
<b>INPUT</b>	<b>HUB</b>		
	ID <sub>max o</sub>	(mm)	19,010
	ID <sub>min o</sub>	(mm)	19,000
	OD <sub>o</sub>	(mm)	36
	E <sub>o</sub>	(N/mm <sup>2</sup> )	80000
	ν <sub>o</sub>	(/)	0,33
	Rz <sub>o</sub>	(/)	0
	<b>SHAFT/PIN</b>		
	OD <sub>max i</sub>	(mm)	19,060
	OD <sub>min i</sub>	(mm)	19,055
	ID <sub>i</sub>	(mm)	0
	E <sub>i</sub>	(N/mm <sup>2</sup> )	210000
	ν <sub>i</sub>	(/)	0,290
	Rz <sub>i</sub>	(/)	0
	l	(mm)	12
	μ <sub>min</sub>	(/)	0,10
μ <sub>max</sub>	(/)	0,15	

Based on the input values we now calculate the minimum and maximum interference  $\delta$  and the radial stresses occurring at the min and max interference by applying Lamé's criterion. The results can be found in table 4, the entire procedure in appendix 8. Next we calculate the torque this press fit can transmit and the force needed to assemble the press fit at the minimum and maximum interference. Lastly we check the von Mises stresses in the case of maximum interference at four points: the inside and the outside diameter of both the pin and the hub. We start by calculating the principal plain stresses:  $\sigma_c$  (circumferential) and  $\sigma_r$  (radial). We do not consider the longitudinal stresses because this is a biaxial stress condition. From table 4 we see that the critical stress location is at the inner diameter of the hub. According to the von Mises yield criterion a material will start to yield when  $\sigma_v$  equals the yield strength  $\sigma_y$ . For the aluminum 7075-T6 of the hub  $\sigma_y = 503 \text{ Mpa}$ <sup>[14]</sup>, which gives us a safety factor of 1,94.

**Table 4.** Output values of the press fit calculation

		Case 1 @20°C	
<b>OUTPUT</b>	$\delta_{min}$	(mm)	0,045
	$\delta_{max}$	(mm)	0,060
	$\sigma_{r, min}$	(N/mm <sup>2</sup> )	79,86
	$\sigma_{r, max}$	(N/mm <sup>2</sup> )	106,48
	T <sub>slip, min</sub>	(Nm)	54,34
	T <sub>slip, max</sub>	(Nm)	108,68
	von Mises stress OD_o	(N/mm <sup>2</sup> )	82,22
	von Mises stress ID_o	(N/mm <sup>2</sup> )	258,92
	von Mises stress OD_i	(N/mm <sup>2</sup> )	106,48
	von Mises stress ID_i	(N/mm <sup>2</sup> )	212,96
	Press-in force min	(kg)	572
Press-in force max	(kg)	1144	

Next we calculate how much the diameters of the pin and the hole change when the temperature changes by using the coefficient of thermal expansion. We then repeat the calculation described above for a temperature of 120°C and -20°C. The results can be found in appendix 8. When the temperature increases by 100°C there is an interference loss of 0,022 mm, because the aluminum hole expands more with temperature than the steel pin. In contrast when the temperature decreases by 40°C, there is an interference increase of 0,009 mm. But even at a temperature of -20°C a safety factor on the stresses of 1,90 remains.

## 10 SPLINE

The main reason high power density and thus low weight can be achieved is the equal load distribution among the planet gears. An unequal load distribution will result in overloaded planet gears, bearings, shafts and carrier.

There are quite some important principles which should be kept in mind during the design concerning the equal load distribution. A small list can be found in the appendix 9a. Most of them can be resolved by proper technical drawings with the correct tolerances.

Apart from these correct tolerances it is crucial to give one of the members (the sun gear, the ring gear or the carrier) the freedom to position itself into its optimal position. The radial component of the gear forces will guide the floating member to its optimal position.

It is possible with the planet configuration to make the fixed ring gear floating, but this is rather complex, a more in depth discussion can be found in appendix 9a.

The most straightforward solution is to make the sun floating with respect to the motor shaft. The motor shaft may only transmit a torque to the sun gear and is not allowed to force the sun gear in a certain position between the planet gears. The radial freedom of the sun gear with respect to the motor is 0,1 mm on the radius. It is large enough to compensate for the worst case misalignment of the centre line of the motor with respect to the centre line of the transmission. This radial play is kept as small as possible to reduce the rotational play to an absolute minimum, namely 0,05 mm. The resulting rotational play of 0,16° on the carrier which is connected to the output shaft through the tripod coupling is negligible.

The spline is designed according to DIN 5480 with the male spline machined according to the norm. The female spline will be made by wire EDM, which gives us the freedom to deviate the female spline profile from the norm and thus achieve our desired radial play.

## 11 SUPPORT STRUCTURE

The support structure displayed in figure 14 provides the alignment of the transmission with respect to the motor.

As previously discussed in section 6 about the advantages of the epicyclic gear reduction, the support structure is only subjected to a torque and the weight of the drivetrain.

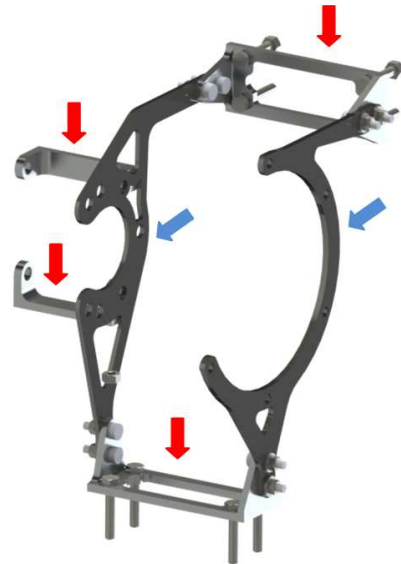


**Figure 14.** Support structure with milled brackets (red) and laser cut mounting parts (blue)

Besides our design goal to make the support structure as light as possible, the design decisions are also influenced by financial considerations: the dimensions of the laser cut parts are about 220 mm x 220 mm, which would result in large and expensive machined parts. To combine inexpensive production with a low weight we decide to laser cut the parts with a stock of 3 mm, which will be machined afterwards to obtain the high tolerances which are necessary to achieve the proper alignment.

The laser cut plates are optimized topologically with software of Altair HyperWorks. Both plates have a similar shape. We can verify these laser cut shapes are indeed the most optimal ones when looking at it as a truss, see figure 15. The torque acting on the central ring is converted into tensile and compression forces, and thus the material is used in the most optimal way.

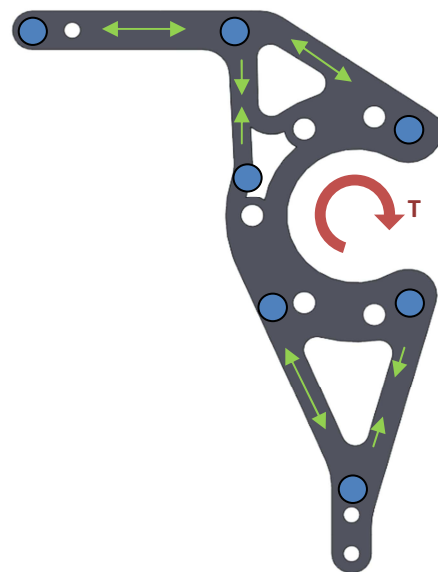


**Figure 15.** Support structure motor considered as a truss. Blue dots represent the hinges connecting beams; the green arrows represent the tensile and compression forces

## 12 TEMPERATURE

The high power density resulting from the very compact and light design of the epicyclic gear reduction does mean we have to check the maximum temperature of each gearbox. The maximum temperature is determined by the oil seal: a temperature higher than  $80^{\circ}\text{C}$ <sup>[15]</sup> will cause damage to the oil seal and can lead to oil leakage.

The temperature increases due to power losses of the gearbox. In this section we will determine the power losses of the meshing gears, the bearings, the oil seals and the churning losses. To calculate the gearbox temperature we search for the gearbox temperature that is needed to dissipate the total power loss by means of convection; the radiation of the motor will be neglected in our calculations and we assume the temperature of the transmission is equal to that of the oil. Despite the fact that our transmissions are fully enclosed in the monocoque, we use a convection coefficient for turbulent ambient air in our calculations:  $100 \frac{\text{W}}{\text{m}^2 \cdot ^{\circ}\text{C}}$ . This is a reasonable assumption since we use three big fans to cool the gearboxes. The total power losses per gearbox are  $P_{\text{loss, total}} = 244 \text{ W}$ , this means a total efficiency of 96,5% per gearbox and an oil temperature of  $T_{\text{oil}} = 58^{\circ}\text{C}$ , which is lower than the maximum allowed temperature (appendix 12). The total power losses can be broken down into four contributors which we discuss more in detail here.

### 12.1 Gear mesh losses

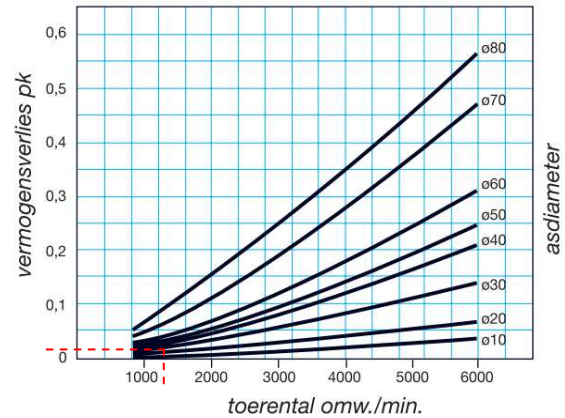
These power losses are due to the combination of the sliding and rolling movement of two teeth in mesh. The planetary reduction has two types of meshes: the sun-planet mesh and the planet-ring mesh. For the sun-planet mesh we calculate a loss of 26,2 W per mesh and an efficiency of 99,6%. The losses at the planet-ring mesh are 6,47 W with an efficiency of 99,7%. The internal gear mesh is more efficient because the sliding velocity along the profile is lower<sup>[16]</sup>: the gears in an internal mesh roll more and glide less compared to an equivalent external mesh. As an input for these calculations we calculated the average power and speed the car will operate in: 14 kW and 1200 rpm. These values are based on logs made on last year's car Eve in 2012-2013, more information can be found in appendix 7a.

### 12.2 Oil seal loss

The oil seal losses are 18,65 W for an input motor shaft speed of 1200 rpm, according to graph 3. This graph is based on friction losses of standard oil seals, used in standard quality oil SAE-30 at  $100^{\circ}\text{C}$  on a grinded shaft after a short period of running in. The graph shows the relation between power loss, shaft diameter and angular velocity.

### 12.3 Bearing losses.

The total bearing losses are 81,7 W, these values are a direct output of the simulations with BEARINX®-online Shaft Calculation as described in section 8.



**Graph 3.** Oil seal power losses in function of the shaft diameter and angular velocity.

### 12.4 Churning losses.

We calculate the churning losses following a method as described in the Ph.D. dissertation by S. Seetharaman<sup>[17]</sup>. We can break the churning losses down into two categories: drag losses and pocketing losses, the former can be further subdivided into three components.

#### 12.4.1 Drag losses:

1. Losses due to oil drag on the periphery of the gear ( $P_{\text{per}}$ ): we calculate these losses for one planet gear, since it has the highest pitch line velocity. We assume the worst case scenario where half of the gear is submerged in oil.  $P_{\text{per}} = 0,403 \text{ W}$ .
2. Losses due to oil drag on the sides of the gear ( $P_{\text{side}}$ ): we make the same assumptions as for the calculation of  $P_{\text{per}}$ . Because we are not sure if we have laminar or turbulent flow on the sides of the planet gear we again calculate the losses assuming the worst possible scenario of laminar flow.  $P_{\text{side}} = 0,487 \text{ W}$ .
3. Losses due to oil filling the teeth cavities ( $P_{\text{cav}}$ ): here we calculate the losses due to oil filling the gear cavities as it rotates in the oil bath. We again assume the gear is submerged halfway into the oil.  $P_{\text{cav}} = 0,005 \text{ W}$ .

#### 12.4.2 Pocketing losses:

These losses are due to squeezing excess oil out of the cavities in the mesh of two mating gears. As two mating gears mesh they enclose a volume that gets smaller as they rotate. The enclosed volume has two end flow areas at the sides of the gear where oil can escape and one backlash flow area between the profiles of the gears where oil can escape.

We start with calculating these flow areas, next we calculate the velocity of the oil escaping through these areas. Using Bernoulli's principle, based on the velocity of the oil escaping, atmospheric pressure and the density of the oil we can then calculate the pressure of the oil escaping at the flow areas. Next we use the conservation of momentum principle to determine the forces acting on the oil as it escapes, which finally leads us to pocketing losses for the planet-ring mesh. We repeat this for the

sun-planet mesh and get a total amount of 45,7 W for the pocketing losses. The pocketing losses are clearly the most influential component of the churning losses.

### 13 CONCLUSION

The result of this thesis is a very compact epicyclic gear reduction with a weight of 2,2 kg, custom designed for the third racecar by Formula Group T. Every component is either produced or sponsored by partner companies who support Formula Group T. This transmission will propel the racecar forwards at the Formula Student competitions where our gear reduction will position amongst the lightest ones compared to other teams. The design judges at the competitions will certainly appreciate the custom design aspect what will benefit our score on the design event. We went through an iterative design process and all mechanical drivetrain components were scrutinized and researched to result in the lightest design possible. This paper is significant research for the long-term vision of Formula Group T to evolve towards building a racecar with four-wheel drive, with in-wheel planetary gearboxes.

### 14 ACKNOWLEDGEMENTS

First and foremost, we would like to thank our supervisor prof. ir. Guido Ceulemans and co-supervisor Giannino Bortolini for sharing their knowledge with us, asking insightful critical questions and guiding us during the design and thesis process. We would also like to give a special thanks to Gerald Camps for his endless engineering support and sharing of knowledge regarding all things gears and beyond, and Willem Vanhoorne from Schaeffler INA FAG for enlightening us with bearing principles. We thank our fellow Formula Group T members for the stimulating discussing and motivating atmosphere they all created that drove us to create this gear reduction. We would also like to express our gratitude to the sponsors of the mechanical drivetrain: E.S. Tooling for milling all parts with great precision, VCST for producing top notch gears, Schaeffler INA FAG for providing all the bearings, SEW-EURODRIVE for their technical and financial support, All Laser Technics for laser cutting parts swiftly, Dichtomatik for providing us with oil seals, Materialise for 3D printing custom C.V. joint boots and Fabory for the much appreciated discount on fasteners. Ultimately a warm thanks to our family for their much needed support and encouragement.

### 15 REFERENCES

- [1] <http://formulagroept.be/>
- [2] <http://events.imeche.org/formula-student/>
- [3] SAE International, 2014 Formula SAE Rules [Online]. Available: <http://students.sae.org/cds/formulaseries/rules/>
- [4] S. Roman, private communication, September 2013.
- [5] A. Peeters, "Modeling of a Vehicle Dynamic Model with Implementation of a Custom Developed Tire Model of a Formula Student Car with LMS International Virtual.Lab Motion Software", M.S. Thesis, Dept. Mech. Eng., Leuven, Belgium, 2013.
- [6] Catalog, Polyurethane Timing Belts, Gates Mectrol GmbH, p. 124-126
- [7] Roloff / Matek Machineonderdelen, 4th edition, D. Muhs, H. Wittel, M. Becker, D. Jannasch, and J. Vossiek, Braunschweig/Wiesbaden, 2010, pp. 579
- [8] Unknown. Elements of Metric Gear Technology [Online].
- [9] Catalog, medias® Product Catalogue, FAG, Schweinfurt, Germany.
- [10] Roloff / Matek Machineonderdelen, 4th edition, D. Muhs, H. Wittel, M. Becker, D. Jannasch, and J. Vossiek, Braunschweig/Wiesbaden, 2010, pp. 656-700
- [11] Catalog No. 9013/AE, Needle Roller Bearing Handbook, NTN Corporation, Osaka, Japan.
- [12] Typical Stribeck curve [Online]. Available: <http://library.nmu.edu/guides/userguides/apacitingtables.htm>
- [13] Fundamentals of Machine Elements, Hamrock et al, McGraw-Hill, 1999
- [14] China jiangyou longhai Special Steel Co , Data Table for: Carbon steel:16MnCr5 , Available: <http://www.steelss.com/Carbon-steel/16mncr5.html>
- [15] Catalog, Technisch handboek Oliekeerringen, ERIKS, Belgium.
- [16] Dudley's Handbook of Practical Gear Design and Manufacture, 2nd ed., S. P. Radzevich, Florida, U.S., 2012, pp. 47-48
- [17] Satya Seetharaman, "An investigation of load-independent power losses of gear systems," Ph.D. dissertation, Dept. Mech. Eng., Ohio State University, Columbus, OH, 2009.